Chemical Physics Letters 608 (2014) 229–234

Contents lists available at ScienceDirect

Chemical Physics Letters

journal homepage: www.elsevier.com/locate/cplett

Photo-less catalysis of TiO_2-reduced graphene oxides

Chunji Jin [a], Xiaoqiang Cui [a], Hongwei Tian [a,*], Xiaoyi Wang [b], Changqing Sun [c], Weitao Zheng [a,*]

[a] Department of Materials Science and Key Laboratory of Automobile Materials of MOE and State Key Laboratory of Superhard Materials, Jilin University, Changchun 130012, China
[b] Key Laboratory of Optical System Advanced Manufacturing Technology, Changchun Institute of Optics, Fine Mechanics and Physics, Chinese Academy of Sciences, Changchun 130033, China
[c] School of Electrical and Electronic Engineering, Nanyang Technological University, Singapore 639798, Singapore

ARTICLE INFO

Article history:
Received 3 March 2014
In final form 5 June 2014
Available online 12 June 2014

ABSTRACT

A series of TiO_2-reduced graphene oxide (RGO) nanocomposites were prepared by a green one-pot hydrothermal reactions using P25 as the titania precursor and graphene oxide (GO). Our method provides the notable advantages of a one-step reaction without employing toxic solvents, thereby providing a green, simple and quick synthetic route to produce TiO_2-RGO nanocomposites. The synthesized nanocomposites showed enhanced photocatalytic activity compared to P25 under UV–vis illumination, it even can degrade the Rhodamine (Rh) B in the dark conditions.

1. Introduction

Degradation of organic pollutants under irradiation of visible light or photo-less has been a great challenge [1]. As an inexpensive and environmentally benign material [2], TiO_2 has been extensively investigated and widely used as a photocatalyst to decompose organic contaminants for drinking water and indoor air purification [3]. However, the photocatalytic activity of TiO_2 is limited by its wide band gap energy (3.2 and 3.0 eV for anatase and rutile phase, respectively), which is only sensitive to the UV light with wavelengths shorter than 380 nm. On the other hand, under solar light irradiation, electron–hole pairs (excitons) can be generated in TiO_2, but the rapid recombination of the photogenerated excitons becomes another factor limiting the efficiency of TiO_2 [4]. Therefore, narrowing the band gap and prolonging the excitons life are the most challenge in the photo-catalytic utilization of TiO_2 though multiple strategies have been developed such as compositing TiO_2 with noble metals, metal oxides and carbonaceous materials [5,6].

The highest fraction of undercoordinated atoms (fewer than that of graphite) and the unusually polarized edge states of Dirac-Fermi polarons (with binding energy at the Fermi level) [7,8], graphene demonstrates extremely high carrier mobility [9–11] and chemical reactivity [12,13]. These emergent attributes enable graphene to be a promising candidate for applications in photocatalysis and bioscience [14,15]. The capability of chemical functionalization and mechanical flexibility also make graphene an ideal mechanical support and charge shuttle for photo sensitizers and catalysts [16].

Much effort has been made to incorporating graphene nanosheets into TiO_2-based composite materials, which have enhanced the photocatalytic activity in a number of studies [17–24]. However, most of the methods are based on nonaqueous synthesis, using agent for reduction or dispersion. In addition to the unsatisfactory catalytic efficiency, the tedious experimental procedure limited their practical applications.

Herein, we report a facile method using green one-pot hydrothermal reaction to prepare TiO_2-RGO nanosheets (TGNS) nanocomposites without any agent being involved. It means that after the hydrothermal course the samples could be separated from the colloidal suspension through centrifugation without any other washing steps. So the course of reaction became much easier and the reaction time was shorter. Most strikingly, the photocatalytic activity of the composites is much higher than the conventional TiO_2 photocatalyst, P25. The composites with the highest photocatalytic ability can even degrade the vast majority of Rh B in 30 min in the dark room conditions. This method of preparation TiO_2-RGO nanocomposites offers a feasible advice for the production of factory. The TGNS composites have great potential for applications in photocatalytic degradation, electrochemical energy storage, and catalyst support and hydrogen evolution.

2. Experimental section

2.1. Materials

Graphite powder, 325 meshes, 99.9995% (metals basis), was obtained from Alfa Aesar to prepare graphene oxide (GO), $NaNO_3$

* Corresponding authors.
E-mail addresses: tianhw@jlu.edu.cn (H. Tian), wtzheng@jlu.edu.cn (W. Zheng).

http://dx.doi.org/10.1016/j.cplett.2014.06.007
0009-2614/

(99.0%), H_2SO_4 (98 wt%), H_2O_2 (30 wt%), HCl (37 wt%), and $KMnO_4$ (99.5%) were obtained from Tianjin Guangfu Chemical Reagent Co. Unless otherwise specified, Rhodamine (Rh B) and other reagents and materials involved were obtained commercially from the Beijing Chemical Reagent Plant (Beijing, China). Deionized water (water purifier, resistivity $\geqslant$18 MΩ cm) was used during the experimental process.

2.2. Preparation of graphene oxide (GO)

GO reduction to graphene and hybridization between TiO_2 nanoparticles and graphene was achieved in a one-step hydrothermal process. GO was prepared from graphite powder using a modified Hummers method [25–27]. In detail, 2 g of graphite was added into a mixture of 1.5 g of $NaNO_3$ and 67.5 ml of concentrated H_2SO_4. Then in the ice-bath condition, 9 g of $KMnO_4$ was added slowly into the mixture. Then we kept the mixture stirred continuously for 12 h in the ice-bath condition. After the ice-bath condition, we kept the mixture stirred continuously for 30 min at 35 °C, then kept the mixture stirred continuously for 12 h at 50 °C, 200 g of ice which made of deionized water was slowly added to dilute the mixture. After that, we stirred the mixture for 2 h, and then 6 ml of 30% H_2O_2 was added slowly till the mixture turn to luminous yellow. After stirred for 2 h, the obtained luminous yellow suspension was exfoliated to produce single layer graphene oxide using a sonicator, and the unexfoliated precipitation was removed by centrifugation. After drying the product in a vacuum drying oven at 60 °C for 24 h, we obtained a brown dispersion of homogeneously exfoliated graphene oxide finally.

2.3. Synthesis of TiO_2-reduced graphene oxide (RGO)

The TiO_2-RGO nanosheets (TGNS) were obtained *via* a hydrothermal method based on Zhang's work with modifications [24]. Briefly, 80 mg of GO dissolved in a solution of distilled H_2O (30 mL) by ultrasonic treatment for 1 h, and 0.1 g of P25 was added to the obtained GO solution and stirred for another 1 h to get a homogeneous suspension. The suspension was then placed in a 40 ml Teflon-sealed autoclave and maintained at 180 °C for 6 h to simultaneously achieve the reduction of GO and the deposition of P25 on the carbon substrate. The ultimate suspension was centrifuged several times and the product was dried at room temperature. We also made some TiO_2-reduced graphene oxide nanocomposites with different content of RGO and different reaction time to analysis the effected factors of photocatalytic performance.

2.4. Synthesis of graphene nanosheets

For comparison, graphene nanosheets (GNS) were obtained by a hydrothermal route under same conditions, but without the addition of P25. Briefly, 30 mg of GO dissolved in a solution of distilled H_2O (30 ml), by ultrasonic treatment for 1 h to get a homogeneous suspension. The suspension was then placed in a 40 ml Teflon-sealed autoclave and maintained at 180 °C for 6 h to simultaneously achieve the GNS. The ultimate suspension was centrifuged several times and the product was dried at 60 °C in vacuum drying oven.

2.5. Characterization

X-ray diffraction (XRD) experiments for the obtained samples were performed to investigate their structures, having a Bragg–Brentano diffractometer (D8 tools) in θ–2θ configuration with a Cu Kα line at 0.15418 nm as a source. The morphology of the products was characterized by scanning electron microscopy (SEM, JEOL JSM-6700F operated at 8 kV), transmission electron microscope and high-resolution transmission electron microscopy (TEM and HRTEM, JEOL JEM-2100F operated at 200 kV). The Raman spectrum was detected with a Renishaw 1000 microspectrometer connected to a Leica microscope with an objective lens of 509 (NA = 0.5). The spectra were obtained under a laser power of 5 mW, an accumulation time of 30 s, and an excitation wavelength of 514.5 nm. The UV–vis absorption spectra were measured on a UV–Vis spectrometer (UV-2500, Shimadzu, Japan). The Brunauer–Emmett–Teller (BET) specific surface areas of the sample powders were measured on ASAP 2020 V3.02 micromeritics surface and porosity analyzer (USA) through nitrogen adsorption. The pH of the Rh B solution was measured on Satorius PB-10 pH meter.

2.6. Measurements of photocatalytic degradation of Rh B

To examine the photocatalytic activity, the photodegradation of Rh B, which is a typical dye resistant to biodegradation, was investigated. A 25 W UV lamp as the light source, 30 mg photocatalyst was suspended, in an aqueous solution (50 mL) of 10 mg L^{-1} Rh B. Prior to the irradiation, the suspensions were magnetically stirred in the dark for 30 min to reach the absorption–desorption equilibrium of the dye on the surface of the photocatalyst. The photocatalytic reaction was started by turning on the UV lamp (the wave crest at 365 nm), and during the photocatalysis, all other lights were insulated and the photocatalytic reactions lasted for 2 h. Aliquots (3 mL) were sampled and filtered through a cellulose filter (0.25 μm) to remove the suspended catalysts. The UV–visible absorption spectrum of the filtered solution was measured using a UV–Vis spectrometer (UV-2500, Shimadzu) and the dye concentration was estimated by recording variations of the maximum absorption band (at 550 nm). The degradation efficiency R (%) can be calculated as:

$$R = (C_0 - C)/C_0 \times 100\%$$

where C_0 is the initial concentration of dye and C is the revised concentration considering dye adsorption on the catalyst after UV irradiation.

2.7. Measurement of pH about the remained Rh B solution

To prove the degradation of Rh B in the dark, we conducted a specific experiment in the dark condition during the whole process, which was similar to the photocatalytic experiment. 30 mg TGNS was added into an aqueous solution (50 mL) of 10 mg L^{-1} Rh B, which was stirring during the whole process in the dark condition. At given intervals (1 h), 7 mL aliquots were sampled and filtered through cellulose filter (0.25 μm) to remove the suspended catalysts. We used the pH meter to test the pH value of the aliquots. After 3 h, we added additional Rh B (0.5 mg) and water (21 mL) into the original mixture solution to ensure there was enough Rh B. Two consecutive cycles were tested.

3. Results and discussion

X-ray diffraction (XRD) measurements, as shown in Figure 1A, confirmed the presence of peaks of GO, P25, and TGNS. The GO peak at $2\theta = 10.4°$ corresponds to a d-spacing of 0.95 nm, which is much larger than that of the natural graphite at 0.335 nm. After hydrothermal treatment of the TGNS, the diffraction patterns of carbon species disappear. XRD profiles confirmed that the composites contain titania in both the anatase and the rutile phases and the TGNS showed a similar XRD pattern to the pure P25. Therefore, the hydrothermal process of the composite synthesis has no obvious impact on the original TiO_2 crystallization.

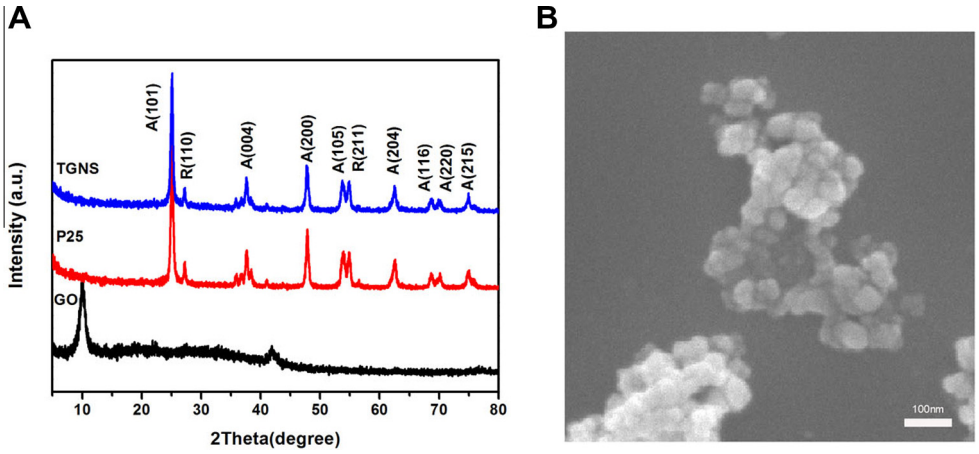

Figure 1. (A) XRD patterns of GO, P25, TGNS and (B) SEM image of TGNS.

Morphological and structural features of the TGNS were examined using scanning and transmission electron microscopy (SEM and TEM). Figures 1B and 2A showed that the TGNS retained the two-dimensional sheet structure with micrometers-long wrinkles after the hydrothermal reduction. Because of the distribution of carboxylic acid groups on the GO, the P25 nanoparticles of 20–30 nm dispersed on the graphene support tend to accumulate along the wrinkles and edges. Figure 2B depicts a high-resolution TEM image of the TGNS. The fringe spacing of 0.37 nm ensures the presence of anatase (101) planes.

Figure 3A shows the Fourier transform infrared spectroscopy (FTIR) of the GO, TiO_2, and TGNS. In the GO spectrum, the broad absorption band centered at 3411 cm^{-1} is attributed to the residual OH groups. The C=O stretching of the COOH groups at edges of the GO sheets is observed at 1731 cm^{-1}. The absorption peak of epoxide groups are observed at 1052 cm^{-1} and 1225 cm^{-1}. The absorption band appearing at 1624 cm^{-1} corresponds to the skeletal vibration of the graphene sheets, indicating the formation of graphene during the hydrothermal reaction. In the TGNS spectrum, the absorption by the C=O group (1731 cm^{-1}) and others decrease obviously in intensity indicates the reduction of GO. In TGNS, all of the trial characteristic peaks imply that the GO was not fully reduced to graphene, and was instead reduced intermediately to a RGO product, which contains residual oxygen-containing groups, such as OH and COOH. For the TGNS, the broad absorption peak at frequency lower than 1000 cm^{-1} was attributed to the vibration of Ti—O—Ti bonds in TiO_2, similar to that presented in P25. However, none of the appreciable difference between the peaks of the TiO_2 and of the TGNS (below 1000 cm^{-1}) has been resolved, which indicates the absence of the Ti—C bond.

Figure 3B shows the Raman spectroscopy of the TGNS synthesized for different reaction duration. The RGO spectra show typical features D band located at 1348 cm^{-1} and G band at 1608 cm^{-1}. G band provided information on the in-plane vibration of sp^2 bonded carbon atoms, while the D band fingerprinted the presence of sp^3 defects in graphene. After hydrothermal treatment at different reaction duration, the positions of these peaks remain unchanged. The D/G intensity ratios change from 0.9 to 1.07 and to 1.09 with reaction duration increasing from 4 h to 6 h and 8 h, respectively. The increase in the D/G intensity ratio indicates a decrease in the average size of the sp^2 domains formed during the hydrothermal reaction. This can be allowed only when newly formed graphitic domains are smaller in size, while more in number as compared to those present in GO before hydrothermal treatment, as reported by Ruoff et al. [28]. All samples show a symmetric 2D and S3 band (Figure S4), a symmetric 2D-band of TGNS at 2699 cm^{-1} implied that RGO is present as a single layer graphene in the nanocomposites [29].

To investigate the porous structures and BET surface areas of the GNS and TGNS samples, the nitrogen adsorption–desorption isotherms and the corresponding pore size distribution curves (inset) were obtained as shown in Figure 4. The nitrogen

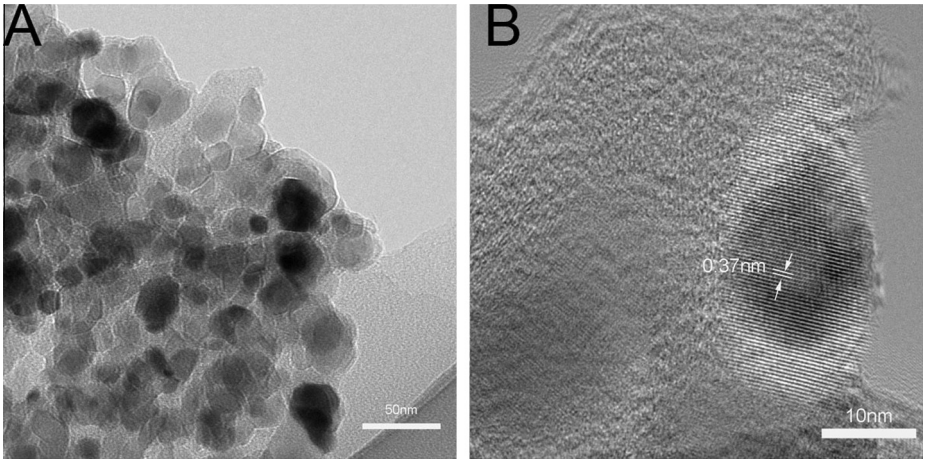

Figure 2. (A) TEM image of TGNS and (B) HRTEM image of TGNS.

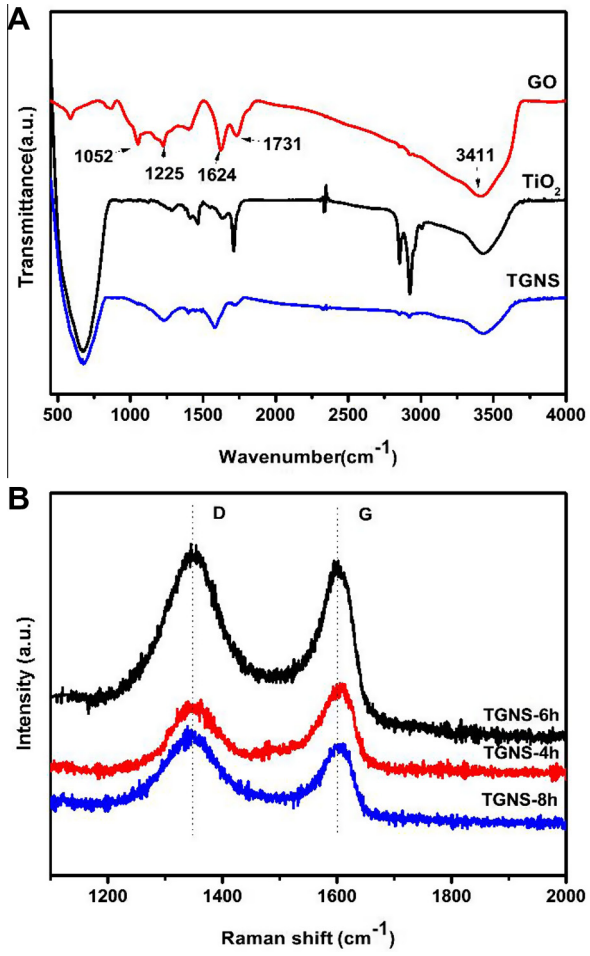

Figure 3. (A) FTIR spectra of GO, TiO_2, and TGNS, (B) Raman spectra of TGNS obtained at different reaction durations.

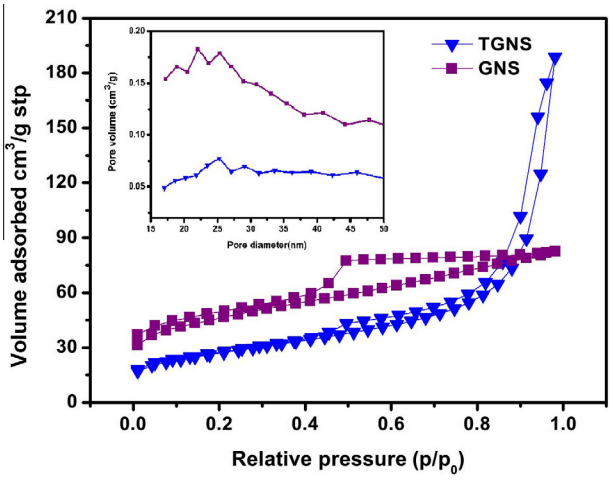

Figure 4. Nitrogen adsorption–desorption isotherms of GNS and TGNS samples. Inset shows the corresponding pore-size distribution plots.

adsorption isotherms of the two samples were not the same. The isotherm of GNS exhibits a type IV with a hysteresis loop according to BDDT classification, reflecting the presence of a mesoporous structure of the sample. The isotherm of TGNS could be classified as type III, typical of nonporous structure. The GNS shows a larger specific surface area (161 $m^2 g^{-1}$) than that of TGNS (96 $m^2 g^{-1}$). The corresponding pore-size distribution curves of GNS and TGNS are depicted in the inset of Figure 4, presenting a peak centered at 22 nm and 25 nm, respectively.

The photocatalytic activity of the specimens was evaluated in terms of the degradation rate of Rh B under UV light excitation. To measure the Rh B concentration in the solution as the time elapsed, a small volume of solution was taken from the dark-aged specimen and the absorbance was measured at the wavelength of 555 nm. The changes of normalized concentration (C/C_0) of the Rh B with irradiation were assumed to be proportional to the normalized maximum absorbance (A/A_0). Prior to photocatalytic experiment, the dye solution with the catalyst was kept in the dark room to attain the absorption–desorption equilibrium of the dye with the catalyst. Figure 5A shows the degradation of the Rh B by the TGNS with different content of GO being stirred in the dark room for 30 min ($t < 0$ region). It was observed that most of the dye molecules remained in the solution of bare P25, whereas a large amount of dye molecules was removed by the TGNS. There are some reasons that may explain the enhanced catalytic of the TGNS nanocomposites. First of all, the enhancement in the photocatalysis should be largely assigned to the great physical adsorption. The BET specific area of TGNS-44% is 96 $m^2 g^{-1}$, the larger specific area can provide more active sites and adsorb more molecules of the dye. Second, the two-dimensional giant π–π conjugation system between Rh B and aromatic regions of the graphene which

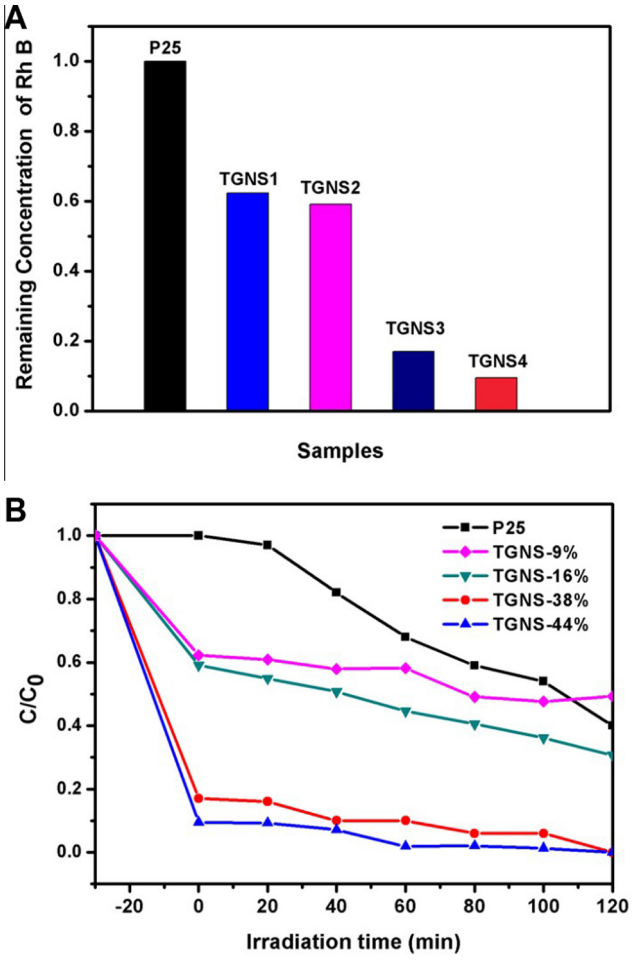

Figure 5. (A) Bar plot showing the remaining relative concentration of Rh B after dark absorption by TGNS1-TGNS4 with different content of RGO, the content of RGO is 9%, 16%, 38% and 44% respectively. (B) Photocatalytic activity of TGNS with different content of RGO. The concentration of Rh B was 10 mg/L.

certainly would lead to a strong adsorption. So the TGNS showed better adsorption of Rh B than the conventional P25 due to its π–π conjugation and the two-dimensional planar structure. Lastly, the RGO in the nanocomposites can act as an electron acceptor, so the photoexcited electrons of TiO_2 in the nanocomposites could be transferred from the conduction band of TiO_2 to RGO quickly, which would make the electron–hole recombination rate decrease. So the photocatalytic activity of TGNS would be higher than P25.

Figure 5B shows that the dye concentration decreases with an increase in the amount of RGO in the solution. The TGNS catalysis proceeds much faster than the conventional P25 and the degradation speed depend on the TGNS concentration. The sample with 44% GO performed best, which removes the Rh B completely within 60 min under UV irradiation. From Figure 5B, the 44% GO sample also shows an excellent degradation performance without light, the solution of Rh B was almost fully degraded by the sample, and only with 10% Rh B remained before UV light excitation. We thought that this phenomenon was not only due to the super adsorbability of graphene, but also due to the degradation ability of TGNS under dark conditions.

To prove above analysis, the dye adsorption ability of P25, mixture of the TiO_2 and graphene, GNS and TGNS were obtained as shown in Figure 6A. It was obvious that, after mixing in the dark for 30 min, most dye molecules remained in the solution with P25 and mixture and more than 70% dye molecules remained with GNS, whereas a large amount of dye molecules (90%) was adsorbed by TGNS. As is well known, the graphene plays an important role in the adsorption of Rh B because of its larger specific surface and strong adsorbed capacity, thus, the more graphene we used the more Rh B should be adsorbed. But it is so strange that the TGNS (with little specific area, 96 $m^2 g^{-1}$) shows the more strong capacity of adsorption than graphene (with larger specific area, 161 $m^2 g^{-1}$). To explore the adsorption of TGNS and GNS, we did another adsorption experiment and the dye concentration was increased 3 times. The adsorption capacity of P25, mixture of P25 and graphene, TGNS and GNS in the dark condition was obtained as shown in Figure 6B. During the four materials put into the Rh B solution for 3 h in the dark condition, the P25 and mixture exhibit much lower adsorption capacity than others, nearly all of the Rh B was remained. While the TGNS and GNS still could adsorb some Rh B, and the adsorption of TGNS was also more than GNS in concentrated dye solution. That means that some dye molecules should be degraded by TGNS under dark condition in addition to adsorption.

To ascertain the photo-less catalysis of TGNS, the measurement of pH value experiments was performed. Under the action of photocatalyst, organic dye would be decomposed into water and carbon dioxide eventually. If the catalytic process happens in the dark condition, the pH of the dye solution should be decreased continuously in the presence of catalyst because of CO_2 was solved in the solution. As shown in Figure 7, the pH values of the Rh B and TGNS mixed solution were decreased gradually as increasing time, this means that some Rh B was decomposed into CO_2 in the dark condition. After 3 h, another amount of dye was added into the mixed solution, the pH values were still decreased as increasing times.

As shown in Figure 6B, the content of Rh B was adequate and the reaction time also was enough to get adsorption–desorption equilibrium, but the content of Rh B was continued decreased. This means that not all of the Rh B was adsorbed, some diminished Rh B should be degraded to a certain extent. In this work, the hydrothermal reaction made the chemical reaction between TiO_2 and graphene, this chemical reaction may be the reason why Rh B could be degraded in the dark condition. As a consequence of the above, besides the physical adsorption of the dye molecules, there may be some other factors which would result to the enhanced catalytic activity such as chemical bonding.

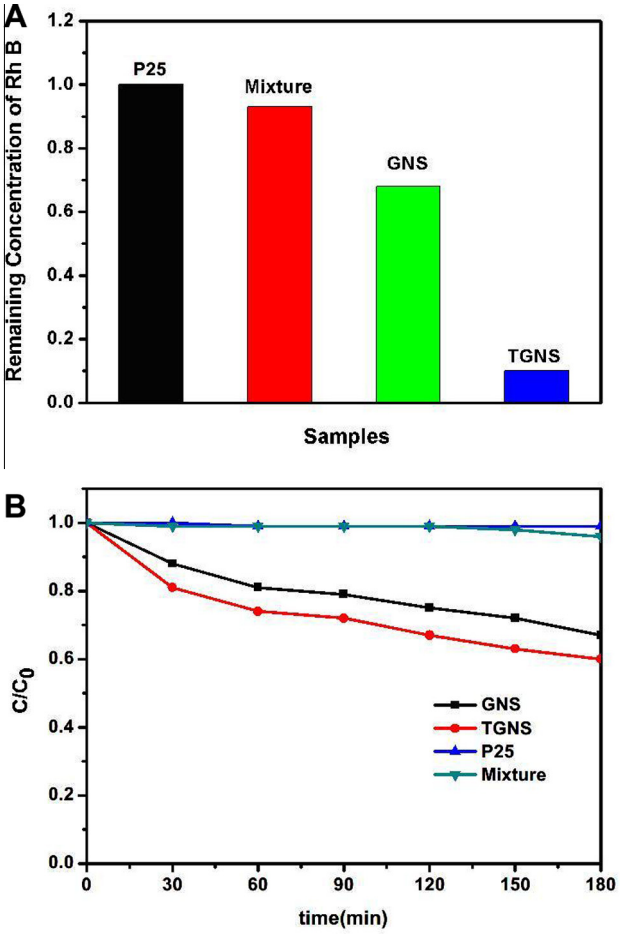

Figure 6. (A) Bar plot showing the remaining relative concentration of Rh B after dark adsorption for 30 min by P25, the mixture of RGO and TiO_2, GNS and TGNS. (B) The adsorption of Rh B in the dark condition with P25, mixture of P25 and graphene which the content of P25 was same to the TGNS, GNS and TGNS. The concentration of the Rh B was 30 mg/L, which was 3 times larger than used in Figure 6A.

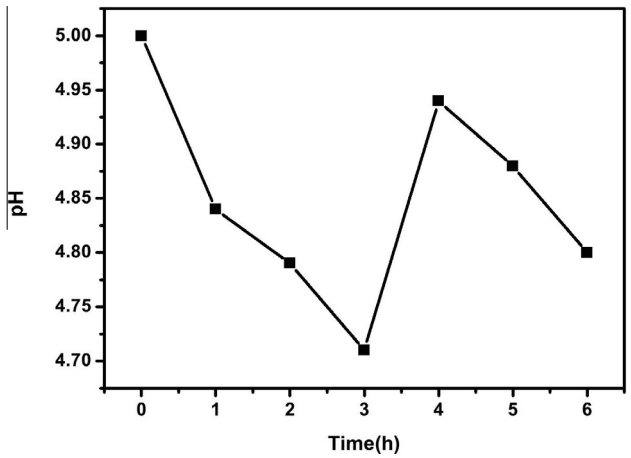

Figure 7. The pH values of Rh B and TGNS mixture solution with a reaction time 6 h in the dark condition.

4. Conclusion

In summary, TGNS with extraordinarily high photocatalytic ability have been synthesized using a more simple hydrothermal reaction method with only water being involved. The best catalytic activity is obtained with 44 wt% RGO at 180 °C reaction temperature for 6 h, which remove Rh B almost completely (only with 10% Rh B remained) without needing UV irradiation. The composites with the highest photocatalytic ability can even degrade the some Rh B in the dark room conditions. This TGNS composite presents a new photo-less catalyst that should find applications in organic pollutant degradation.

Acknowledgement

This work was supported by the National Natural Science Foundation of China (No. 51372095) and Natural Science Foundation of Jilin Province (No. 20140101107JC).

References

[1] M.R. Hoffmann, S.T. Martin, W.Y. Choi, D.W. Bahnemannt, Chem. Rev. 95 (1995) 69.
[2] H.S. Kim, W.T. Moon, Y.K. Jun, S.H. Hong, Sensors Actuat. B – Chem. 120 (2006) 63.
[3] J. Zhang, Q. Xu, Z. Feng, M. Li, C. Li, Angew. Chem. Int. Ed. 47 (2008) 1766.
[4] J.W. Tang, J.R. Durrant, D.R. Klug, J. Am. Chem. Soc. 130 (2008) 13885.
[5] P.F. Fu, P.Y. Zhang, Appl. Catal. B 96 (2010) 176.
[6] Z.Y. Zhong, Y.D. Yin, B. Gates, Y.N. Xia, Adv. Mater. 12 (2000) 206.
[7] C.Q. Sun, Nanoscale 2 (2010) 1930.
[8] X.Y. Zhang, Y.G. Nie, W.T. Zheng, J.L. Kuo, C.Q. Sun, Carbon 49 (2011) 3615.
[9] A.K. Geim, K.S. Novoselov, Nat. Mater. 6 (2007) 183.
[10] H. Chen, M.B. Muller, K.J. Gilmore, G.G. Wallace, D. Li, Adv. Mater. 20 (2008) 3557.
[11] D.Y. Pan, J.C. Zhang, Z. Li, M.H. Wu, Adv. Mater. 22 (2010) 734.
[12] Y.Y. Liang, H.L. Wang, H.S. Casalongue, Z. Chen, H.J. Dai, Nano Res. 3 (2010) 701.
[13] W.T. Zheng, C.Q. Sun, Energy & Environ. Sci. 4 (2011) 627.
[14] C.X. Guo, H.B. Yang, Z.M. Sheng, Z.S. Lu, Q.L. Song, C.M. Li, Angew. Chem. Int. Ed. 49 (2010) 3014.
[15] Z. Liu, J.T. Robinson, X.M. Sun, H.J. Dai, J. Am. Chem. Soc. 130 (2008) 10876.
[16] V.P. Kamat, J. Phys. Chem. Lett. 2 (2011) 242.
[17] S.J. Ding, J.S. Chen, D.Y. Luan, F.Y.C. Boey, S. Madhavibc, X.W. Lou, Chem. Commun. 47 (2011) 5780.
[18] C.Z. Zhu, S.J. Guo, P. Wang, L. Xing, Y.X. Fang, Y.M. Zhai, S.J. Dong, Chem. Commun. 46 (2010) 7148.
[19] B. Li et al., Chem. Commun. 46 (2010) 3499.
[20] M.S.A.S. Shah, A.R. Park, K. Zhang, J.H. Park, P.J. Yoo, ACS Appl. Mater. Interfaces 4 (2012) 3893.
[21] F. Wang, K. Zhang, J. Mol. Catal. A – Chem. 345 (2011) 101.
[22] Q. Xiang, J.G. Yu, M. Jaroniec, Chem. Soc. Rev. 41 (2012) 782.
[23] X. An, J.C. Yu, RSC Adv. 1 (2012) 1426.
[24] H. Zhang, X.J. Lv, Y.M. Li, Y. Wang, J.H. Li, ACS Nano 4 (2010) 380.
[25] W.S. Hummers, R.E. Offeman, J. Am. Chem. Soc. 80 (1958) 1339.
[26] Y. Wang, Y.M. Li, L.H. Tang, J. Lu, J.H. Li, Electrochem. Commun. 11 (2009) 889.
[27] D.C. Marcano et al., ACS Nano 4 (2010) 4806.
[28] S. Stankovich et al., Carbon 45 (2007) 1558.
[29] O. Akhavan, M. Abdolahad, A. Esfandiar, M. Mohatashamifar, J. Phys. Chem. C 114 (2010) 12955.